Interplay between adsorbate diffusion and electron tunneling at an insulating surface

Keith McKenna,* Thomas Trevethan, and Alexander Shluger
World Premier International Research Center, Advanced Institute for Materials Research, Tohoku University, 2-1-1, Katahira, Aoba-ku, Sendai 980-8577, Japan
and Department of Physics and Astronomy, University College London, Gower Street, London WC1E 6BT, United Kingdom
(Received 15 July 2010; published 18 August 2010)

We investigate electron tunneling between defects and mobile adsorbates on the surface of MgO and show that electrons can be transferred to Au and Pt atoms from defects, such as oxygen vacancies, over distances ~20 Å even at room temperature. As a result of the surface-mediated interaction following electron transfer, the mobility of these metal atoms is enhanced significantly. Such processes may affect the kinetics of growth and structure of adsorbed clusters and thin films and the interaction of molecules with surfaces.

DOI: 10.1103/PhysRevB.82.085427 PACS number(s): 68.43.Jk, 82.20.Gk, 82.30.Fi

I. INTRODUCTION

In wide gap insulators there are a large number of surface defects that may serve as sources of electrons for approaching atoms or molecules. These defects are created during sample preparation as well as a result of photon and electron irradiation (see, for example, Refs. 1–4). Electron transfer from surface defects to adsorbing atoms and molecules is of considerable fundamental interest and importance for applications such as gas sensing, solar cells, and molecular electronics.[5–7] Electron transfer has been shown to be important in the adsorption and diffusion of oxygen molecules on TiO_2 and SnO_2 surfaces[5,8] and may affect the adsorption of organic molecules on insulating surfaces.[9,10] Electron transfer has also been implicated in mechanisms of metal oxidation[11] and used to explain the luminescence observed during molecular adsorption at surfaces.[12]

The electron transfer can take place either by tunneling to incoming or already adsorbed molecules [see Figs. 1(a) and 1(b)] or as a result of direct contact between donor and acceptor. For example, the electron tunneling between surface F^+ centers and V^- centers stabilized in the bulk of CaO nanoparticles at low temperatures has been studied in Ref. 13 using electron paramagnetic resonance. But generally, direct observations of distant electron tunneling are rare as many experimental methods, such as scanning probe microscopies (SPM) often used in these studies, are quite slow and observe the surface in (local) equilibrium. Therefore, it is difficult to directly monitor the dynamics of atoms and electrons and conclusions are often drawn on the basis of modeling the kinetics of growth of surface structures or chemical reactions. As a result, the role electron tunneling from defects at oxide surfaces in the growth of metal nanoclusters and in catalysis has not been well understood. Unravelling the potential implications of this effect is important given the widespread use of oxides as substrates.

In particular, it is known that catalytic properties of metal nanoparticles on oxide substrates depend on the size and shape of the particles[14,15] and are strongly affected by surface defects.[16,17] Therefore, there is a strong ongoing effort to control the nucleation and growth kinetics of metal clusters on a surface by atom deposition. To understand and guide the experimental measurements, the nucleation kinetics of metal clusters on point defects are often modeled using a mean-field theory[16–18] and kinetic Monte Carlo simulations (see, for example, Refs. 19 and 20). These simulations, however, ignore the possibility of long-range electron tunneling between defects and adsorbing metal atoms. There is a great deal of experimental evidence showing that deposited metal atoms become charged, e.g., by defects such as oxygen vacancies, at the MgO surface.[3,4,21,22] But the usual adiabatic explanation is that atoms are first deposited onto the surface in a neutral state and subsequently diffuse to the most stable adsorption sites, at a rate that depends on the temperature. Once adsorbed near an electron donor, such as an oxygen vacancy, electron density spills onto the metal atom.[23]

In this paper, we take the adsorption and diffusion of metal atoms on the MgO surface as an example and show by theoretical calculations that long-range electron tunneling from defects makes the dynamics of metal atoms deposited onto insulating surfaces much more complex than is often assumed. Our calculations show that, complementary to the adiabatic picture, electron tunneling from defects can occur over distances of up to 20 Å and following the electron transfer the mobility of the metal atom is enhanced significantly. This example illustrates how the dynamics of metal atoms on metal-oxide surfaces results from a complex interplay between atomic diffusion and electron tunneling, and these effects should also be more generally important for other atomic and molecular species.

II. METHODS OF CALCULATIONS

There is an extensive literature concerned with modeling long-range electron transfer between molecules in solvents

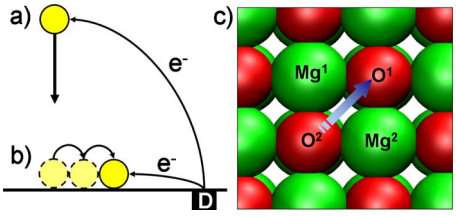

FIG. 1. (Color online) Illustration showing electron transfer from surface defects to metal atoms (a) during approach and (b) following adsorption and diffusion on the surface. (c) Adsorption sites for metal atoms on the MgO(001) surface.

because of its relevance to biological processes[24] as well as in solids[25] and in nanosystems.[7] There are also relevant examples in the solid state, such as electron transfer between color centers in insulators,[26] between surfaces and adsorbed acceptor molecules[27] and calculations of the mobility of polarons.[28] However, theoretically modeling electron transfer is still challenging due to the fact that standard quantum mechanical approaches, such as density-functional theory (DFT), often fail to describe systems comprised of several open subsystems among which the electron numbers may fluctuate.[29,30] The importance of this effect for calculations of long-range charge transfer is well known[31] and approaches to rectify the problem, such as constrained DFT,[32,33] have been proposed. Here, we employ an alternative approach (described below) which divides the donor-acceptor system into individual subsystems and then introduces a simple model for their interaction.

At a surface, the energetics of electron transfer is governed by an interplay between three energy terms: the ionization potential (IP) of an electron donor (e.g., a defect), the electron affinity (EA) of an electron acceptor (e.g., a metal atom) and the change in the interaction energy (ΔIE) between the donor and acceptor following the charge transfer

$$\Delta G = IP - EA + \Delta IE. \tag{1}$$

Here we approximate ΔIE by a screened electrostatic interaction in the following way:

$$\Delta IE = \frac{e^2}{4\pi\epsilon_{\text{eff}} d}(q_{\text{A}} - q_{\text{D}} - 1), \tag{2}$$

where q_{D} and q_{A} are the charge of the donor and acceptor before electron transfer, d is their separation, and ϵ_{eff} is the effective dielectric screening constant. If the donor is at the surface and the acceptor is vertically above it [Fig. 1(a)], or if the donor and acceptor are both close to the surface but separated laterally [Fig. 1(b)], ϵ_{eff} takes a particularly simple form: $\epsilon_{\text{eff}}=(\epsilon_{\text{MgO}}+\epsilon_{\text{vac}})/2$. This expression is derived from classical electrostatics by considering a charge above a dielectric surface and the corresponding induced image charge in the dielectric.[34] In the results presented in this paper we employ this approximation together with the experimental values for MgO [$\epsilon_{\text{MgO}}(0)=9.7$ and $\epsilon_{\text{MgO}}(\infty)=2.9$]. The bulk dielectric constant calculated using density functional perturbation theory within a periodic approach is very similar (3.2 for the electronic part and 10.2 for the full dielectric constant). Whether it is the static or optical dielectric constant that is used depends on the time scale over which the dielectric surface responds to the electric field. We note, however, that these approximations may not be valid for more complicated cases of defects and adsorbates at, e.g., steps or kinks where the surface screening properties will be reduced even further (see, for example, discussion in Refs. 35 and 36).

The calculations of metal atom adsorption energies, IPs and EAs are carried out using an embedded cluster method (see Ref. 37 for a detailed description). For the calculation of these properties the embedded cluster approach is appropriate as the structural perturbation is well localized around the defect or the adsorbed metal atom while the long-range polarization induced by charged species is well described by the classical shell model. In our calculations the MgO surface is represented by a cubic MgO nanoparticle with 5 nm edge length. The quantum cluster for the ideal surface contains 52 ions treated at an all-electron level with 6–31G basis sets for Mg and O. This quantum cluster was chosen by incrementally increasing the number of quantum mechanically treated ions until the calculated properties were converged. In order to prevent spurious spilling of the wave function from the quantum cluster into the classically modeled regions, first- and second-nearest-neighbor Mg ions are modeled using a semilocal effective core pseudopotential possessing no associated basis functions. This type of approach has been employed previously in many other embedded cluster calculations (e.g., see Refs. 23 and 37–41). The core electrons of Au, Pt, and Pd atoms are replaced by LANL pseudopotentials and the valence electrons are treated using the LANL08 basis set.[42] This revised basis set has triple-ζ valence quality compared to the double-ζ LANL2DZ basis sets that were previously commonly used with this pseudopotential. The positions of all ions within 10 Å from the center of the quantum cluster are optimized self-consistently. We used the B3LYP hybrid density functional, which has been shown by previous studies to perform much better than the local density approximation, generalized gradient approximation, or Hartree-Fock approaches for describing the structure and electronic properties of wide gap insulators (e.g., see Refs. 43–46. For MgO, in particular, B3LYP performs exceptionally well and there are many examples in the literature where very good agreement with experiment has been obtained (e.g., see Refs. 37 and 47–49). We also note that the calculated EAs of free metal atoms using this method are underestimated by no more than 0.15 eV compared to experiment.

In the diabatic limit the rate at which the electron transfer reaction $\text{Me}^0+D^{q_{\text{D}}} \rightarrow \text{Me}^- + D^{q_{\text{D}}+1}$ proceeds may be approximated by[7,24]

$$k_{et} = \frac{2\pi}{\hbar}|H_{AB}|^2 \frac{1}{\sqrt{4\pi\lambda k_{\text{B}} T}} \exp\left(-\frac{E_{\text{act}}}{k_{\text{B}} T}\right), \tag{3}$$

where Me is a metal atom, D is an electron donor, E_{act} is the activation energy, and H_{AB} is the matrix element for electron transfer at nuclear coordinates corresponding to the crossing point of diabatic potential energy surfaces. The activation energy is given by

$$E_{\text{act}} = \frac{(\lambda + \Delta G)^2}{4\lambda}, \tag{4}$$

where the reorganization energy, λ, is defined in the usual way.[24]

Fully quantum mechanical calculation of electron tunneling matrix elements is extremely challenging and the few examples in the literature concern electron tunneling between equivalent sites.[28] The situation here is much more complicated and so we take a widely used approach by approximating the electron tunneling matrix elements by a simple exponential, $H_{AB}=A\exp(-\beta d/2)$. This dependence is observed experimentally and theoretically for many different systems.[25] We use values of $\beta=1.4$ Å^{-1} and $A=2.7$ eV typi-

TABLE I. Ionization potential and charge (q_D) of electron donors on the MgO surface. Detailed descriptions of the structure and properties of these defects can be found in the references listed in the table.

Defect	q_D	IP_v	IP_r	Refs.
$Mg_{3C}+e^-$	−1	1.25	0.64	This work, 39
$H@O_{5C}$	0	2.0–2.4	1.2	This work, 38
F_s^0	0	3.1–3.4	2.2–2.5	This work, 37 and 59
H@RC	0	4.76	3.07	40
F_s^+	1	4.9	3.8	This work, 59
O_{3C}	0	5.1–5.7	4.2	37 and 39

cal for a barrier height ~2 eV (Ref. 50) although we have checked that using a larger value of β does not qualitatively affect our results.[51]

III. RESULTS OF CALCULATIONS

On the MgO surface there are many different types of defects which may serve as electron donors and these have been the subject of numerous theoretical and experimental investigations.[37,52–58] High concentrations of such defects are known to exist in powders and can also be created by reaction with molecules and by irradiation.[38] In Table I we summarize the vertical (i.e., including only electronic polarization) and fully relaxed (including also ionic relaxation) IPs of a number of potential electron donors on the MgO surface. These include electrons trapped by three-coordinated Mg ions ($Mg_{3C}+e^-$), hydrogen atoms adsorbed on the O site of the MgO(001) surface and at a reverse corner ($H@O_{5C}$ and H@RC), neutral and positively charged surface oxygen vacancies (F_s^0 and F_s^+) and a three-coordinated O ions (O_{3C}). In the cases where previous calculations exist we include the relevant reference in the table and if there is more than one calculation the full range of values are shown.

As electron acceptors we have considered Au, Pd, and Pt atoms. However, for clarity our results will be discussed in detail for the particular example of Au atoms interacting with a defective MgO surface. We first consider the possibility that electron transfer occurs as the neutral Au atom approaches the surface during deposition [Fig. 1(a)] before considering its adsorption and diffusion on the surface in the vicinity of defects [Fig. 1(b)]. To evaluate k_{et} at room temperature we use the calculated EA of the free Au atom (2.18 eV) and the IPs from Table I. We use the optical dielectric constant as this is relevant for typical atom velocities (~100 ms^{-1}) where only the electronic screening response should be considered (e.g., see Ref. 60). We find that the highest transfer rates are from neutral oxygen vacancies and that any atom landing within 7 Å of a surface vacancy will be charged during its approach. Assuming a uniform flux of Au atoms and a concentration of surface vacancies ~10^{13} cm^{-2} (although the actual concentration depends on how the surface is produced and processed) we estimate that about 16% of Au atoms will be charged before collision with the surface. After collision with the surface the Au atom or ion (if charged) may either recoil or stick to the surface, in the process exciting phonons. The possibility that the Au ion scatters from the surface following charge transfer, carrying the electron with it, may be measurable by electron paramagnetic resonance spectroscopy and atom scattering experiments.[61]

TABLE II. Calculated properties of Au, Pd, and Pt atoms. For all neutral atoms considered adsorption on the O site of the MgO surface is lowest in energy. † following electron trapping and full ionic relaxation this atom moves to the Mg site.

	Au	Pd	Pt
E_{ad}	−0.76	−1.13	−1.84
EA_v	0.58	0.00	0.09
EA_r	2.02†	0.87	1.07
E_b^0	0.49	0.43	1.12
E_b^-	0.17	0.33	0.44

We now consider what happens if an Au atom or ion collides and sticks to the MgO surface. To do this we calculate the adsorption energies (E_{ad}), vertical and relaxed electron affinities (EA_v and EA_r) and barriers to diffusion in both charge states (E_b^0 and E_b^-). This data is summarized in Table II and the results have been corrected for basis set superposition error. The calculated properties are found to be similar to those calculated previously, where comparisons are available. For example, previous calculations of the neutral Au atom adsorption energy find values between −0.89 and −1.01 eV (Refs. 62 and 63) compared to −0.76 eV in our work. A previous calculation of the neutral Au diffusion barrier obtained 0.27 eV (Ref. 64) compared to 0.17 eV here. There have been numerous calculations of the Pd adsorption energy ranging between −1.0 and −1.5 eV (Refs. 63 and 65–68), and our value of −1.13 eV falls within this range. A previous calculation of the neutral Pd diffusion barrier obtained 0.4 eV (Ref. 65) which is also very close to our calculated value. Our calculations show that negatively charged Au prefers adsorption on the magnesium site but all other atoms and ions considered prefer the oxygen site. If we consider the case that the atom sticks to the surface in the neutral charge state, we can again use Eq. (3) to compute the electron transfer rates between defects and the adsorbed metal atom. In this case we use the static MgO dielectric constant and the calculated EA at the surface. Figure 2 shows the calculated electron transfer rate at room temperature for the three shallowest electron donors in Table I. The electron transfer rates decay exponentially with separation but can exceed 10^5 Hz even at distances ~15 Å at room temperature.

For Au^0 the barrier to diffusion is 0.49 eV and the path is in the (110) direction between O sites [Fig. 1(c)]. Following the electron transfer Au^- relaxes onto the Mg site and the barrier to diffusion is reduced from 0.49 to 0.17 eV. The diffusion path is in the (110) direction [e.g., $Mg^1 \rightarrow Mg^2$ in Fig. 1(c)]. This significant reduction in the barrier to diffusion suggests that electron transfer can strongly influence the dynamics of metal atoms on the MgO surface. For instance, assuming an Arrhenius dependence with a prefactor of

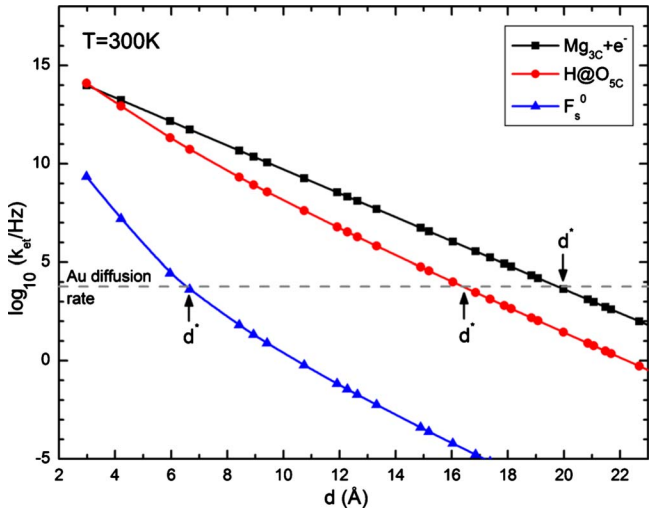

FIG. 2. (Color online) Calculated electron transfer rates between surface defects and an adsorbed Au atom at room temperature. The horizontal line represents the rate for Au hopping between adjacent oxygen sites.

10^{12} Hz, the Au hopping rate at room temperature is increased from 6×10^{3} Hz to 6×10^{8} Hz (an increase of 10^{5}) following electron transfer. To characterize the spatial extent of the influence of a given defect on metal atom dynamics one can define a separation d^{*}, below which the electron transfer rate k_{et} is faster than the neutral atom hopping rate (as indicated in Fig. 2). This idea is conceptually similar to the black sphere model for tunneling recombination of defects.[26] Figure 3 shows how d^{*} depends on the temperature for shallowest electron donor defects. For example, at room temperature, $d^{*}=20.0$ Å for the $Mg_{3C}+e^{-}$ defect, $d^{*}=16.4$ Å for $H@O_{5C}$ and $d^{*}=6.6$ Å for the F_s^0 defect. F_s^0 has a very weak temperature dependence because in this case the activation energies for electron transfer and diffusion are quite similar.

Following charge transfer, the high mobility of Au^{-} means it is able to rapidly diffuse to the most stable binding

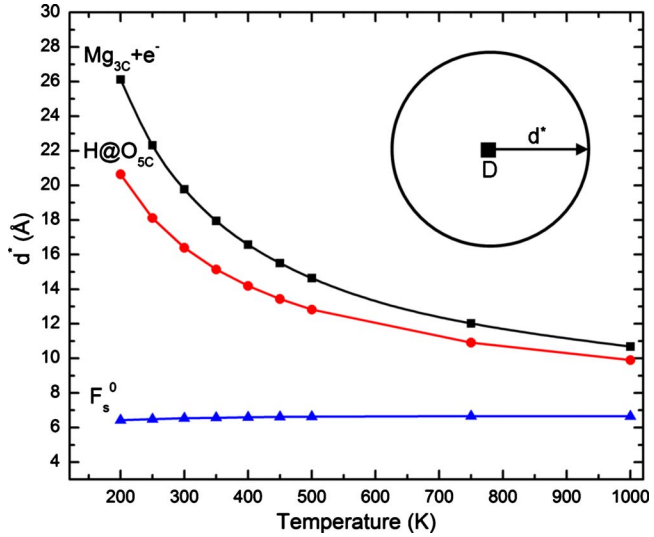

FIG. 3. (Color online) The calculated distance, d^{*}, at which the electron transfer rate is equal to the Au hopping rate.

sites. In general, the most stable sites need not be related to the original donor defect. However, for H and F_s^0, electrostatic attraction will favor the association of the now oppositely charged defect and metal atom. The particular case of F_s has been discussed in detail previously and the equilibrium configuration involves the Au atom adsorbed directly above the vacancy.[23] Similar to the well-known harpooning reactions in molecules,[69] this mechanism allows the surface vacancy to harpoon the metal atom and draw it closer. We have calculated the IP of the F_s-Au complex and find that it is smaller than that of the isolated F_s center by about 1 eV, therefore, subsequent charge transfer becomes even more favorable.

These results indicate that long-range electron transfer can encourage metal clusters to nucleate at surface vacancies at much lower temperatures that would be possible without it. We find similar effects for Pt, where even at 500 K electron transfer is faster than the Pt hopping rate for separations ~20 Å. This has an even more dramatic effect on dynamics than for Au owing to the much lower mobility of neutral Pt. For example, the Pt hopping rate at 500 K is ~5 Hz which is increased by nearly seven orders of magnitude following electron transfer. Pd, on the other hand, has a much smaller electron affinity making charge transfer much less important for dynamics.

IV. DISCUSSION AND CONCLUSION

The examples presented above illustrate how electron tunneling can affect the dynamics of adsorbed species at insulating surfaces, such as atoms, clusters, and molecules. There are also many potential sources of electrons, such as hydrogen-related defects and defects segregated to grain boundaries and dislocations in polycrystalline films.[70] For the metal atoms we have considered, mobility is enhanced by electron transfer from defects but in other cases electron transfer may hinder diffusion or even stimulate desorption. Moreover, surfaces with lower dielectric constant, such as alumina, can be expected to show stronger effects.

Electron transfer at insulating surfaces has previously been used to interpret the diffusion of oxygen molecules on TiO_2,[8] ion scattering experiments on insulating surfaces,[61] adsorboluminescence,[12] and defect recombination kinetics in insulators.[26] In the latter cases, luminescence studies can provide a test for theoretical models. Probing directly the dynamics of atoms and molecules at insulating surfaces, however, is more challenging as commonly used tools, such as SPM, provide only a snapshot of the system. The ability to both influence and detect electron transfer processes using a scanning probe tip has been demonstrated theoretically.[71]

In summary, we have shown how defects on oxide surfaces can serve as sources of electrons which can be transferred over distances up to 20 Å to acceptors, such as adsorbed metal atoms. Charge transfer can modify the mobility of species on the surface significantly and change the nature of interaction with the donor. Such effects may affect the kinetics of growth of nanoscale clusters[16] and thin films and should be included in atomistic simulations.[19] They can be also studied using atom scattering, adsorboluminescence and Kelvin probe microscopy.[4]

ACKNOWLEDGMENTS

We acknowledge helpful discussions with T. Harker, J. Blumberger, and C. Barth. This work was supported by the Ministry of Education, Culture, Sports, Science with Grant-in-Aid for Young Scientists (B) under Project No. 22740192. Computer resources on the Hector service were provided via our membership of the U.K.'s HPC Materials Chemistry Consortium and funded by EPSRC (portfolio Grant No. EP/F067496).

*k.mckenna@ucl.ac.uk

[1] V. E. Henrich and P. A. Cox, Appl. Surf. Sci. **72**, 277 (1993).
[2] M. Frank, M. Bäumer, R. Kühnemuth, and H.-J. Freund, J. Phys. Chem. B **105**, 8569 (2001).
[3] M. Sterrer, T. Risse, U. M. Pozzoni, L. Giordano, M. Heyde, H.-P. Rust, G. Pacchioni, and H.-J. Freund, Phys. Rev. Lett. **98**, 096107 (2007).
[4] C. Barth and C. R. Henry, J. Phys. Chem. C **113**, 247 (2009).
[5] A. Gurlo, ChemPhysChem **7**, 2041 (2006).
[6] J. L. Brédas, D. Beljonne, V. Coropceanu, and J. Cornil, Chem. Rev. **104**, 4971 (2004).
[7] D. M. Adams *et al.*, J. Phys. Chem. B **107**, 6668 (2003).
[8] E. Wahlström, E. K. Vestergaard, R. Schaub, A. Rønnau, M. Vestergaard, E. Lægsgaard, I. Stensgaard, and F. Besenbacher, Science **303**, 511 (2004).
[9] T. Trevethan and A. L. Shluger, J. Phys. Chem. C **111**, 15375 (2007).
[10] L. A. Zimmerli, Ph.D. thesis, University of Basel, 2007.
[11] C. Ocal, S. Ferrer, and N. García, Surf. Sci. **163**, 335 (1985).
[12] V. T. Coon, Surf. Sci. **88**, L42 (1979).
[13] Y. I. Aristov, V. N. Parmon, and K. I. Zamaraev, React. Kinet. Catal. Lett. **27**, 245 (1985).
[14] M. Che and C. O. Bennett, Adv. Catal. **36**, 55 (1989).
[15] C. R. Henry, Prog. Surf. Sci. **80**, 92 (2005).
[16] G. Haas, A. Menck, H. Brune, J. V. Barth, J. A. Venables, and K. Kern, Phys. Rev. B **61**, 11105 (2000).
[17] C. Barth and C. R. Henry, Phys. Rev. Lett. **91**, 196102 (2003).
[18] J. A. Venables, L. Giordano, and J. H. Harding, J. Phys.: Condens. Matter **18**, S411 (2006).
[19] L. Xu, C. T. Campbell, H. Jónsson, and G. Henkelman, Surf. Sci. **601**, 3133 (2007).
[20] G. Sitja, R. O. Uñac, and C. R. Henry, Surf. Sci. **604**, 404 (2010).
[21] B. Yoon, H. Häkkinen, U. Landman, A. S. Wörz, J.-M. Antonietti, S. Abbet, K. Judai, and U. Heiz, Science **307**, 403 (2005).
[22] J. A. Farmer, N. Ruzycki, J. F. Zhu, and C. T. Campbell, Phys. Rev. B **80**, 035418 (2009).
[23] A. M. Ferrari and G. Pacchioni, J. Phys. Chem. **100**, 9032 (1996).
[24] R. A. Marcus and N. Sutin, Biochim. Biophys. Acta **811**, 265 (1985).
[25] K. V. Mikkelsen and M. A. Ratner, Chem. Rev. **87**, 113 (1987).
[26] E. Kotomin and V. Kuzovkov, Rep. Prog. Phys. **55**, 2079 (1992).
[27] Y. I. Aristov, A. I. Volkov, V. N. Parmon, and K. I. Zamaraev, React. Kinet. Catal. Lett. **25**, 329 (1984).
[28] N. A. Deskins and M. Dupuis, J. Phys. Chem. C **113**, 346 (2009).
[29] A. Ruzsinszky, J. P. Perdew, G. I. Csonka, O. A. Vydrov, and G. E. Scuseria, J. Chem. Phys. **125**, 194112 (2006).
[30] J. P. Perdew, A. Ruzsinszky, L. A. Constantin, J. Sun, and G. I. Csonka, J. Chem. Theory Comput. **5**, 902 (2009).
[31] D. J. Tozer, J. Chem. Phys. **119**, 12697 (2003).
[32] Q. Wu and T. V. Voorhis, J. Chem. Phys. **125**, 164105 (2006).
[33] H. Oberhofer and J. Blumberger, J. Chem. Phys. **131**, 064101 (2009).
[34] J. D. Jackson, *Classical Electrodynamics*, 2nd ed. (Wiley, New York, 1975).
[35] P. Ebert, X. Chen, M. Heinrich, M. Simon, K. Urban, and M. G. Lagally, Phys. Rev. Lett. **76**, 2089 (1996).
[36] R. Slavchov, T. Ivanov, and B. Radoev, J. Phys.: Condens. Matter **19**, 226005 (2007).
[37] P. V. Sushko, A. L. Shluger, and C. R. A. Catlow, Surf. Sci. **450**, 153 (2000).
[38] M. Sterrer, T. Berger, O. Diwald, E. Knözinger, P. V. Sushko, and A. L. Shluger, J. Chem. Phys. **123**, 064714 (2005).
[39] K. P. McKenna, P. V. Sushko, and A. L. Shluger, J. Am. Chem. Soc. **129**, 8600 (2007).
[40] D. Ricci, C. Di Valentin, G. Pacchioni, P. V. Sushko, A. L. Shluger, and E. Giamello, J. Am. Chem. Soc. **125**, 738 (2003).
[41] A. L. Shluger, K. P. McKenna, P. V. Sushko, D. Muñoz Ramo, and A. V. Kimmel, Model. Simul. Mater. Sci. Eng. **17**, 084004 (2009).
[42] L. E. Roy, P. J. Hay, and R. L. Martin, J. Chem. Theory Comput. **4**, 1029 (2008).
[43] A. Wander and N. M. Harrison, Surf. Sci. **457**, L342 (2000).
[44] T. Bredow and A. R. Gerson, Phys. Rev. B **61**, 5194 (2000).
[45] J. Muscat, A. Wander, and N. M. Harrison, Chem. Phys. Lett. **342**, 397 (2001).
[46] J. Robertson, K. Xiong, and S. J. Clark, Thin Solid Films **496**, 1 (2006).
[47] O. Diwald, M. Sterrer, E. Knözinger, P. V. Sushko, and A. L. Shluger, J. Chem. Phys. **116**, 1707 (2002).
[48] J. C. Lian, E. Finazzi, C. Di Valentin, T. Risse, H.-J. Gao, G. Pacchioni, and H.-J. Freund, Chem. Phys. Lett. **450**, 308 (2008).
[49] F. Napoli, M. Chiesa, E. Giamello, C. Di Valentin, F. Gallino, and G. Pacchioni, J. Phys. Chem. C **114**, 5187 (2010).
[50] J. J. Hopfield, Proc. Natl. Acad. Sci. U.S.A. **71**, 3640 (1974).
[51] For example, on increasing β to 2.5 Å, d^* for Au and the $Mg_{3C}+e^-$ defect is decreased to 11.5 Å at 300 K.
[52] E. Giamello, M. C. Paganini, D. M. Murphy, A. M. Ferrari, and G. Pacchioni, J. Phys. Chem. B **101**, 971 (1997).
[53] L. Ojamäe and C. Pisani, J. Chem. Phys. **109**, 10984 (1998).
[54] P. V. Sushko, J. L. Gavartin, and A. L. Shluger, J. Phys. Chem. B **106**, 2269 (2002).
[55] D. Ricci, G. Pacchioni, P. V. Sushko, and A. L. Shluger, J. Chem. Phys. **117**, 2844 (2002).
[56] M. Chiesa, M. C. Paganini, E. Giamello, C. D. Valentin, and G. Pacchioni, Angew. Chem., Int. Ed. **42**, 1759 (2003).
[57] M. Chiesa, M. C. Paganini, G. Spoto, E. Giamello, C. D. Valen-

tin, A. D. Vitto, and G. Pacchioni, J. Phys. Chem. B **109**, 7314 (2005).
[58] M. Chiesa, M. C. Paganini, E. Giamello, D. M. Murphy, C. D. Valentin, and G. Pacchioni, Acc. Chem. Res. **39**, 861 (2006).
[59] T. König, G. H. Simon, H.-P. Rust, G. Pacchioni, M. Heyde, and H.-J. Freund, J. Am. Chem. Soc. **131**, 17544 (2009).
[60] A. G. Borisov and V. A. Esaulov, J. Phys.: Condens. Matter **12**, R177 (2000).
[61] C. Auth, A. G. Borisov, and H. Winter, Phys. Rev. Lett. **75**, 2292 (1995).
[62] A. Del Vitto, G. Pacchioni, F. Delbecq, and P. Sautet, J. Phys. Chem. B **109**, 8040 (2005).
[63] G. Pacchioni, L. Giordano, and M. Baistrocchi, Phys. Rev. Lett. **94**, 226104 (2005).
[64] G. Pacchioni, S. Sicolo, C. D. Valentin, M. Chiesa, and E. Giamello, J. Am. Chem. Soc. **130**, 8690 (2008).
[65] S. Sicolo and G. Pacchioni, Surf. Sci. **602**, 2801 (2008).
[66] J. Goniakowski, Phys. Rev. B **58**, 1189 (1998).
[67] A. V. Matveev, K. M. Neyman, I. V. Yudanov, and N. Rösch, Surf. Sci. **426**, 123 (1999).
[68] L. Giordano, C. Di Valentin, J. Goniakowski, and G. Pacchioni, Phys. Rev. Lett. **92**, 096105 (2004).
[69] R. S. Mulliken, J. Am. Chem. Soc. **74**, 811 (1952).
[70] K. P. McKenna and A. L. Shluger, Phys. Rev. B **79**, 224116 (2009).
[71] T. Trevethan and A. Shluger, Nanotechnology **20**, 264019 (2009).